

# Evolutionary Algorithms Applied to Multi-Objective Aerodynamic Shape Optimization

Alfredo Arias-Montaña<sup>†</sup>, Carlos A. Coello Coello<sup>†\*</sup> and Efrén Mezura-Montes<sup>‡</sup>

**Abstract** Optimization problems in many industrial applications are very hard to solve. Many examples of them can be found in the design of aeronautical systems. In this field, the designer is frequently faced with the problem of considering not only a single design objective, but several of them, i.e., the designer needs to solve a Multi-Objective Optimization Problem (MOP). In aeronautical systems design, aerodynamics plays a key role in aircraft design, as well as in the design of propulsion system components, such as turbine engines. Thus, aerodynamic shape optimization is a crucial task, and has been extensively studied and developed. Multi-Objective Evolutionary Algorithms (MOEAs) have gained popularity in recent years as optimization methods in this area, mainly because of their simplicity, their ease of use and their suitability to be coupled to specialized numerical simulation tools. In this chapter, we will review some of the most relevant research on the use of MOEAs to solve multi-objective and/or multi-disciplinary aerodynamic shape optimization problems. In this review, we will highlight some of the benefits and drawbacks of the use of MOEAs, as compared to traditional design optimization methods. In the second part of the chapter, we will present a case study on the application of MOEAs for the solution of a multi-objective aerodynamic shape optimization problem.

---

<sup>†</sup>CINVESTAV-IPN (Evolutionary Computation Group), Departamento de Computación, Av. IPN No. 2508, Col. San Pedro Zacatenco, México D.F. 07360, MEXICO. e-mail: aarias@computacion.cs.cinvestav.mx, ccoello@cs.cinvestav.mx

<sup>‡</sup>Laboratorio Nacional de Informática Avanzada (LANIA A.C.), Rébsamen 80, Centro, Xalapa, Veracruz, 91000, MEXICO. e-mail: emezura@lania.mx

\* The second author is also affiliated to the UMI LAFMIA 3175 CNRS at CINVESTAV-IPN.

## 1 Introduction

There are many industrial areas in which optimization processes help to find new solutions and/or to increase the performance of an existing one. Thus, in many cases a research goal can be translated into an optimization problem. Optimal design in aeronautical engineering is, by nature, a multiobjective, multidisciplinary and highly difficult problem. Aerodynamics, structures, propulsion, acoustics, manufacturing and economics, are some of the disciplines involved in this type of problems. In fact, even if a single discipline is considered, many design problems in aeronautical engineering have conflicting objectives (e.g., to optimize a wing's lift and drag or a wing's structural strength and weight). The increasing demand for optimal and robust designs, driven by economics and environmental constraints, along with the advances in computational intelligence and the increasing computing power, has improved the role of computational simulations, from being just analysis tools to becoming design optimization tools.

In spite of the fact that gradient-based numerical optimization methods have been successfully applied in a variety of aeronautical/aerospace design problems,<sup>2</sup> [30, 16, 42] their use is considered a challenge due to the following difficulties found in practice:

1. The design space is frequently multimodal and highly non-linear.
2. Evaluating the objective function (performance) for the design candidates is usually time consuming, due mainly to the high fidelity and high dimensionality required in the simulations.
3. By themselves, single-discipline optimizations may provide solutions which not necessarily satisfy objectives and/or constraints considered in other disciplines.
4. The complexity of the sensitivity analyses in Multidisciplinary Design Optimization (MDO<sup>3</sup>) increases as the number of disciplines involved becomes larger.
5. In MDO, a trade-off solution, or a set of them, are searched for.

Based on the previously indicated difficulties, designers have been motivated to use alternative optimization techniques such as Evolutionary Algorithms (EAs) [31, 20, 33]. Multi-Objective Evolutionary Algorithms (MOEAs) have gained an increasing popularity as numerical optimization tools in aeronautical and aerospace engineering during the last few years [1, 21]. These population-based methods mimic the evolution of species and the survival of the fittest, and compared to traditional optimization techniques, they present the following advantages:

- (a) *Robustness*: In practice, they produce good approximations to optimal sets of solutions, even in problems with very large and complex design spaces, and are less prone to get trapped in local optima.

---

<sup>2</sup> It is worth noting that most of the applications using gradient-based methods have adopted them to find global optima or a single compromise solution for multi-objective problems.

<sup>3</sup> Multidisciplinary Design Optimization, by its nature, can be considered as a multi-objective optimization problem, where each discipline aims to optimize a particular performance metric.

- (b) *Multiple Solutions per Run*: As MOEAs use a population of candidates, they are designed to generate multiple trade-off solutions in a single run.
- (c) *Easy to Parallelize*: The design candidates in a MOEA population, at each generation, can be evaluated in parallel using diverse paradigms.
- (d) *Simplicity*: MOEAs use only the objective function values for each design candidate. They do not require a substantial modification or complex interfacing for using a CFD (Computational Fluid Dynamics) or CSD/M (Computational Structural Dynamics/Mechanics) code.
- (e) *Easy to hybridize*: Along with the simplicity previously stated, MOEAs also allow an easy hybridization with alternative methods, e.g., memetic algorithms, which additionally introduce specificities to the implementation, without influencing the MOEA simplicity.
- (f) *Novel Solutions*: In many cases, gradient-based optimization techniques converge to designs which have little variation even if produced with very different initial setups. In contrast, the inherent explorative capabilities of MOEAs allow them to produce, some times, novel and non-intuitive designs.

An important volume of information has been published on the use of MOEAs in aeronautical engineering applications (mainly motivated by the advantages previously addressed). In this chapter, we provide a review of some representative works, dealing specifically with multi-objective aerodynamic shape optimization.

The remainder of this chapter is organized as follows: In Section 2, we present some basic concepts and definitions adopted in multi-objective optimization. Next, in Section 3, we review some of the work done in the area of multi-objective aerodynamic shape optimization. This review covers: *surrogate based optimization*, *hybrid MOEA optimization*, *robust design optimization*, *multidisciplinary design optimization*, and *data mining and knowledge extraction*. In Section 4 we present a case study and, finally, in Section 5. we present our conclusions and final remarks.

## 2 Basic Concepts

A Multi-Objective Optimization Problem (MOP) can be mathematically defined as follows<sup>4</sup>:

$$\text{minimize } \mathbf{f}(\mathbf{x}) := [f_1(\mathbf{x}), f_2(\mathbf{x}), \dots, f_k(\mathbf{x})] \quad (1)$$

subject to:

$$g_i(\mathbf{x}) \leq 0 \quad i = 1, 2, \dots, m \quad (2)$$

$$h_i(\mathbf{x}) = 0 \quad i = 1, 2, \dots, p \quad (3)$$

---

<sup>4</sup> Without loss of generality, minimization is assumed in the following definitions, since any maximization problem can be transformed into a minimization one.

where  $\mathbf{x} = [x_1, x_2, \dots, x_n]^T$  is the vector of decision variables, which are bounded by lower ( $x_i^l$ ) and upper ( $x_i^u$ ) limits which define the search space  $\mathcal{S}$ ,  $f_i : \mathbf{R}^n \rightarrow \mathbf{R}$ ,  $i = 1, \dots, k$  are the objective functions and  $g_i, h_j : \mathbf{R}^n \rightarrow \mathbf{R}$ ,  $i = 1, \dots, m$ ,  $j = 1, \dots, p$  are the constraint functions of the problem.

In other words, we aim to determine from among the set  $\mathcal{F} \subseteq \mathcal{S}$  ( $\mathcal{F}$  is the feasible region of the search space  $\mathcal{S}$ ) of all vectors which satisfy the constraints, those that yield the optimum values for all the  $k$  objective functions, simultaneously. The set of constraints of the problem defines  $\mathcal{F}$ . Any vector of variables  $\mathbf{x}$  which satisfies all the constraints is considered a feasible solution. In their original version, an EA (and also a MOEA) lacks a mechanism to deal with constrained search spaces. This has motivated a considerable amount of research regarding the design and implementation of constraint-handling techniques for both EAs and MOEAs [10, 29].

## 2.1 Pareto dominance

Pareto dominance is an important component of the notion of optimality in MOPs and is formally defined as follows:

**Definition 1.** A vector of decision variables  $\mathbf{x} \in \mathbf{R}^n$  dominates another vector of decision variables  $\mathbf{y} \in \mathbf{R}^n$ , (denoted by  $\mathbf{x} \preceq \mathbf{y}$ ) if and only if  $\mathbf{x}$  is partially less than  $\mathbf{y}$ , i.e.  $\forall i \in \{1, \dots, k\}, f_i(\mathbf{x}) \leq f_i(\mathbf{y}) \wedge \exists i \in \{1, \dots, k\} : f_i(\mathbf{x}) < f_i(\mathbf{y})$ .

**Definition 2.** A vector of decision variables  $\mathbf{x} \in \mathcal{X} \subset \mathbf{R}^n$  is **nondominated** with respect to  $\mathcal{X}$ , if there does not exist another  $\mathbf{x}' \in \mathcal{X}$  such that  $\mathbf{f}(\mathbf{x}') \preceq \mathbf{f}(\mathbf{x})$ .

In order to say that a solution dominates another one, it needs to be strictly better in at least one objective, and not worse in any of them.

## 2.2 Pareto optimality

The formal definition of *Pareto optimality* is provided next:

**Definition 3.** A vector of decision variables  $\mathbf{x}^* \in \mathcal{F} \subseteq \mathcal{S} \subset \mathbf{R}^n$  is **Pareto optimal** if it is nondominated with respect to  $\mathcal{F}$ .

In words, this definition says that  $\mathbf{x}^*$  is Pareto optimal if there exists no feasible vector  $\mathbf{x}$  which would decrease some objective without causing a simultaneous increase in at least one other objective (assuming minimization). This definition does not provide us a single solution (in decision variable space), but a set of solutions which form the so-called *Pareto Optimal Set* ( $\mathcal{P}^*$ ), whose formal definition is given

by:

**Definition 4.** The **Pareto optimal set**  $\mathcal{P}^*$  is defined by:

$$\mathcal{P}^* = \{\mathbf{x} \in \mathcal{F} | \mathbf{x} \text{ is Pareto optimal}\}$$

The vectors that correspond to the solutions included in the Pareto optimal set are said to be *nondominated*.

### 2.3 Pareto front

When all nondominated solutions are plotted in objective function space, the non-dominated vectors are collectively known as the *Pareto front* ( $\mathcal{PF}^*$ ).

**Definition 5.** The **Pareto front**  $\mathcal{PF}^*$  is defined by:

$$\mathcal{PF}^* = \{\mathbf{f}(\mathbf{x}) \in \mathbf{R}^k | \mathbf{x} \in \mathcal{P}^*\}$$

The goal on a MOP consists on determining  $\mathcal{P}^*$  from  $\mathcal{F}$  of all the decision variable vectors that satisfy (2) and (3). Thus, when solving a MOP, we aim to find not one, but a set of solutions representing the best possible trade-offs among the objectives (the so-called Pareto optimal set).

## 3 Multi-Objective Aerodynamic Shape Optimization

### 3.1 Problem definition

Aerodynamics is the science that deals with the interactions of fluid flows and objects. This interaction is governed by conservation laws which are mathematically expressed by means of the *Navier-Stokes* equations, which comprise a set of partial differential equations, being unsteady, nonlinear and coupled among them. Aerodynamicists are interested in the effects of this interaction, in terms of their aerodynamic forces and moments, which are the result of integrating the pressure and shear stresses distributions that the flow exerts over the object with which it is interacting. In its early days, aerodynamic designs were done by extensive use of experimental facilities. Nowadays, the use of Computational Fluid Dynamics (CFD) technology to simulate the flow of complete aircraft configurations, has made it possible to obtain very impressive results with the help of high performance computers and fast numerical algorithms. At the same time, experimental verifications are carried out in scaled flight tests, avoiding many of the inherent disadvantages

and extremely high costs of wind tunnel technology. Therefore, we can consider aerodynamics as a mature engineering science.

Thus, current aerodynamic research focuses on finding new designs and/or improving current ones, by using numerical optimization techniques. In the case of multi-objective optimization, the objective functions are defined in terms of aerodynamic coefficients and/or flow conditions. Additionally, design constraints are included to render the solutions practical or realizable in terms of manufacturing and/or operating conditions. Optimization is accomplished by means of a more or less systematic variation of the design variables which parameterize the shape to be optimized. A variety of optimization algorithms, ranging from gradient-based methods to stochastic approaches with highly sophisticated schemes for the adaptation of the individual mutation step sizes, are currently available. From them, MOEAs have been found to be a powerful but easy-to-use choice. Next, we will briefly review some of the most representative works on the use of MOEAs for aerodynamic design. The review comprises the following dimensions that are identified as the most relevant, from a practical point of view, for the purposes of this chapter:

- Surrogate-based optimization,
- Hybrid MOEA optimization,
- Robust design optimization,
- Multidisciplinary design-optimization, and
- Data-mining and knowledge extraction.

### 3.2 *Surrogate-based optimization*

Evolutionary algorithms, being population-based algorithms, often require population sizes, and a number of evolution steps (generations) that might demand tremendous amounts of computing resources. Examples of these conditions are presented by Benini [4], who reported computational times of 2000 hrs. in the multi-objective re-design of a transonic turbine rotor blade, using a population with 20 design candidates, and 100 generations of evolution time, in a four-processors workstation. Thus, when expensive function evaluations are required, the required CPU time may turn prohibitive the application of MOEAs, even with today's available computing power.

For tackling the above problem, one common technique adopted in the field of aerodynamic shape optimization problems, is the use of surrogate models. These models are built to approximate computationally expensive functions. The main objective in constructing these models is to provide a reasonably accurate approximation to the real functions, while reducing by several orders of magnitude the computational cost. Surrogate models range from Response Surface Methods (RSM) based on low-order polynomial functions, Gaussian processes or Kriging, Radial Basis Functions (RBFs), Artificial Neural Networks (ANNs), to Support Vector Machines (SVMs). A detailed description of each of these techniques is beyond the

scope of this chapter, but the interested reader is referred to Jin [19] for a comprehensive review of these and other approximation techniques.

In the context of aerodynamic shape optimization problems, some researchers have used surrogate models to reduce the computational time used in the optimization process. The following is a review of some representative research that has been conducted in this area:

- Lian and Liou [26] addressed the multi-objective optimization of a three-dimensional rotor blade, namely the redesign of the NASA rotor 67 compressor blade, a transonic axial-flow fan rotor. Two objectives were considered in this case: (i) maximization of the stage pressure rise, and (ii) minimization of the entropy generation. Constraints were imposed on the mass flow rate to have a difference less than 0.1% between the new one and the reference design. The blade geometry was constructed from airfoil shapes defined at four span stations, with a total of 32 design variables. The authors adopted a MOEA based on MOGA [14] with real numbers encoding. The optimization process was coupled to a second-order RSM, which was built with 1,024 design candidates using the Improved Hypercube Sampling (IHS) algorithm. The authors reported that the evaluation of the 1,024 sampling individuals took approximately 128 hours (5.33 days) using eight processors and a Reynolds-Averaged Navier-Stokes CFD simulation. In their experiments, 12 design solutions were selected from the RSM-Pareto front obtained, and such solutions were verified with a high fidelity CFD simulation. The objective function values slightly differed from those obtained by the approximation model, but all the selected solutions were better in both objective functions than the reference design.
- Song and Keane [46] performed the shape optimization of a civil aircraft engine nacelle. The primary goal of the study was to identify the trade-off between aerodynamic performance and noise effects associated with various geometric features for the nacelle. For this, two objective functions were defined: i) scarf angle, and ii) total pressure recovery. The nacelle geometry was modeled using 40 parameters, from which 33 were considered design variables. In their study, the authors implemented the NSGA-II [12] as the multi-objective search engine, while a commercial CFD software was used for evaluation of the three-dimensional flow characteristics. A kriging-based surrogate model was adopted in order to keep the number of designs being evaluated with the CFD tool to a minimum. In their experiments, the authors reported difficulties in obtaining a reliable Pareto front (there were large discrepancies between two consecutive Pareto front approximations). They attributed this behavior to the large number of variables in the design problem, and also to the associated difficulties to obtain an accurate kriging model for these situations. In order to alleviate this, they performed an analysis of variance (ANOVA) test to find the variables that contributed the most to the objective functions. After this test, they presented results with a reduced surrogate model, employing only 7 decision variables. The authors argued that they obtained a design similar to the previous one, but requiring a lower computational cost because of the use of a reduced number of variables in the kriging model.

- Arabnia and Ghaly [2] presented the aerodynamic shape optimization of turbine stages in three-dimensional fluid flow, so as to minimize the adverse effects of three-dimensional flow features on the turbine performance. Two objectives were considered: (i) maximization of isentropic efficiency for the stage, and (ii) minimization of the streamwise vorticity. Additionally, constraints were imposed on: (1) inlet total pressure and temperature, (2) exit pressure, (3) axial chord and spacing, (4) inlet and exit flow angles, and (5) mass flow rate. The blade geometry, both for rotor and stator blades, was based on the E/TU-3 turbine which is used as a reference design to compare the optimization results. The multi-objective optimization consisted of finding the best distribution of 2D blade sections in the radial and circumferential directions. The authors adopted NSGA [47] as their search engine. Both objective functions were evaluated using a 3D CFD flow simulation, taking an amount of time of 10 hours per design candidate. The authors adopted an artificial neural network (ANN) based model. The ANN model with backpropagation, contained a single hidden layer with 50 nodes, and was trained and tested with 23 CFD simulations, sampling the design space using the Latin Hypercubes technique. The optimization process was undertaken by using the ANN model to estimate both the objective functions, and the constraints. Finally, the nondominated solutions obtained were evaluated with the actual CFD flow simulation. The authors indicated that they were able to obtain design solutions which were better than the reference turbine design.

### 3.2.1 Comments regarding surrogate-based optimization

The accuracy of the surrogate model relies on the number and on the distribution of samples provided in the search space, as well as on the selection of the appropriate model to represent the objective functions and constraints. One important fact is that Pareto-optimal solutions based on the computationally cheap surrogate model do not necessarily satisfy the real CFD evaluation. So, as indicated in the previous references, it is necessary to verify the whole set of Pareto-optimal solutions found from the surrogate, which can render the problem very time consuming. If discrepancies are large, this condition might attenuate the benefit of using a surrogate model. The verification process is also needed in order to update the surrogate model. This latter condition raises the question of how often in the design process it is necessary to update the surrogate model. There are no general rules for this, and many researchers rely on previous experiences and trial and error guesses.

CFD analyses rely on discretization of the flow domain and in numerical models of the flow equations. In both cases, some sort of reduced model can be used as fitness approximation methods, which can be further used to generate a surrogate model. For example, Lee et al. [24] use different grid resolutions for the CFD simulations. Coarse grids are used for global exploration, while fine grids are used for solution exploitation purposes.

Finally, many of the approaches using surrogates, build them, relating the design variables with the objective functions. However, Leifsson and Koziel [25], have re-



cently proposed the use of physics-based surrogate models in which, they are built relating the design variables with pressure distributions (instead of objective functions). The premise behind this approach is that in aerodynamics, the objective functions are not directly related with the design variables, but with the pressure distributions. The authors have presented successful results using this new kind of surrogate model for global transonic airfoil optimization. Its extension to multiobjective aerodynamic shape optimization is straightforward and very promising.

### 3.3 Hybrid MOEA optimization

One of the major drawbacks of MOEAs is that they are very demanding (in terms of computational time), due to the relatively high number of objective function evaluations that they typically require. This has motivated a number of approaches to improve their efficiency. One of them consists in hybridizing a MOEA with a gradient-based method. In general, gradient-based methods converge quickly for simple topologies of the objective functions but will get trapped in a local optimum if multi-modal objective functions are considered. In contrast, MOEAs can normally avoid local minima and can also cope with complex, noisy objective function topologies. The basic idea behind this hybridization is to resort to gradient-based methods, whenever the MOEA convergence is slow. Some representative works using this idea are the following:

- Lian et al. [27] deal with a multi-objective redesign of the shape blade of a single-stage centrifugal compressor. The objectives are: (i) to maximize the total head, and (ii) to minimize the input power at a design point. These objectives are conflicting with each other. In their hybrid approach, they couple a gradient-based method that uses a Sequential Quadratic Programming (SQP) scheme, with a GA-based MOEA. The SQP approach works in a confined region of the design space where a surrogate model is constructed, and optimized with gradient-based methods. In the hybrid approach of this example, the MOEA is used as a global search engine, while the SQP model is used as a local search mechanism. Both mechanisms are alternatively used under a trust-region framework until Pareto optimal solutions are obtained. By this hybridization approach, favorable characteristics of both global and local search are maintained.
- Chung et al. [9] address a multidisciplinary problem involving supersonic business jet design. The main objective of this particular problem was to obtain a trade-off design having good aerodynamic performances while minimizing the intensity of the sonic boom signature at the ground level. Multiobjective optimization was used to obtain trade-offs among the objective functions of the problem which were to minimize: (i) the aircraft drag coefficient, (ii) initial pressure rise (boom overpressure), and (iii) ground perceived noise level. In this study, the authors proposed and tested the Gradient Enhanced Multiobjective Genetic Algorithm (GEMOGA). The basic idea of this MOEA is to enhance the non-dominated solutions obtained by a genetic algorithm with a gradient-based local

search procedure. One important feature of this approach was that the gradient information was obtained from the Kriging model. Therefore, the computational cost was not considerably increased.

- Ray and Tsai [38] considered a multiobjective transonic airfoil shape design optimization problem with two objectives to be minimized: (i) the ratio of the drag to lift squared coefficients, and (ii) the squared moment coefficient. Constraints were imposed on the flow Mach number and angle of attack. The MOEA used is a multi-objective particle swarm optimizer (MOPSO). This MOEA was also hybridized with a gradient-based algorithm. Contrary to standard hybridization schemes where gradient-based algorithms are used to improve the nondominated solutions obtained (i.e., as a local search engine), in this approach the authors used the gradient information to repair solutions not satisfying the equality constraints defined in the problem. This repairing algorithm was based on the Marquardt-Levenberg algorithm. During the repairing process, a subset of the design variables was used, instead of the whole set, in order to reduce the dimensionality of the optimization problem to be solved.

### 3.3.1 Comments on hybrid MOEA optimization

Experience has shown that hybridizing MOEAs with gradient-based techniques can, to some extent, increase their convergence rate. However, in the examples presented above, the gradient information relies on local and/or global surrogate models. For this, one major concern is how to build a high-fidelity surrogate model with the existing designs in the current population, since, their distribution in the design space can introduce some undesired bias in the surrogate model. Additionally, there are no rules for choosing the number of points for building the surrogate model, nor for defining the number of local searches to be performed. These parameters are empirically chosen. Another idea that has not been explored in multi-objective evolutionary optimization, is to use adjoint-based CFD solutions to obtain gradient information. Adjoint-based methods are also mature techniques currently used for single objective aerodynamic optimization [28], and gradient information with these techniques can be obtained with as much of an additional objective function evaluation.

## 3.4 Robust design optimization

In aerodynamic optimization, uncertainties in the environment must be taken into account. For example, the operating velocity of an aircraft may deviate from the normal condition during the flight. This change in velocity can be so high that it changes the Mach and/or Reynolds number for the flow. The variation of these parameters can substantially change the aerodynamic properties of the design. In this case, a robust optimal solution is desired, instead of the optimal solution found for

ideal operating conditions. By robustness, it is meant in general that the performance of an optimal solution should be insensitive to small perturbations of the design variables or environmental parameters. In multiobjective optimization, the robustness of a solution can be an important factor for a decision maker in choosing the final solution. Search for robust solutions can be treated as a multiobjective task, i.e., to maximize the performance and the robustness simultaneously. These two tasks are very likely conflicting, and therefore, MOEAs can be employed to find a number of trade-off solutions. In the context of multi-objective aerodynamic shape optimization problems, we summarize next some work on robust design.

- Yamaguchi and Arima [51] dealt with the multi-objective optimization of a transonic compressor stator blade in which three objectives were minimized: (i) pressure loss coefficient, (ii) deviation outflow angle, and (iii) incidence toughness. The last objective function can be considered as a robust condition for the design, since it is computed as the average of the pressure loss coefficients at two off-design incidence angles. The airfoil blade geometry was defined by twelve design variables. The authors adopted MOGA [14] with real-numbers encoding as their search engine. Aerodynamic performance evaluation for the compressor blade was done using Navier-Stokes CFD simulations. The optimization process was parallelized using 24 processors in order to reduce the computational time required.
- Rai [37] dealt with the robust optimal aerodynamical design of a turbine blade airfoil shape, taking into account the performance degradation due to manufacturing uncertainties. The objectives considered were: (i) to minimize the variance of the pressure distribution over the airfoil's surface, and (ii) to maximize the probability of constraint satisfaction. Only one constraint was considered, related to the minimum thickness of the airfoil shape. The author adopted a multi-objective version of the differential evolution algorithm and used a high-fidelity CFD simulation on a perturbed airfoil geometry in order to evaluate the aerodynamic characteristics of the airfoil generated by the MOEA. The geometry used in the simulation was perturbed, following a probability density function that is observed for manufacturing tolerances. This process had a high computational cost, which the author reduced using a neural network surrogate model.
- Shimoyama et al. [44] applied a design for multi-objective six-sigma (DFMOSS) [43] for the robust aerodynamic airfoil design of a Mars exploratory airplane. The aim is to find the trade-off between the optimality of the design and its robustness. The idea of the DFMOSS methodology was to incorporate a MOEA to simultaneously optimize the mean value of an objective function, while minimizing its standard deviation due to the uncertainties in the operating environment. The airfoil shape optimization problems considered two cases: a robust design of (a) airfoil aerodynamic efficiency (lift to drag ratio), and (b) airfoil pitching moment constraint. In both cases, only the variability in the flow Mach number was taken into account. The authors adopted MOGA [14] as their search engine. The airfoil geometry was defined with 12 design variables. The aerodynamic performance of the airfoil was evaluated by CFD simulations using the Favre-Averaged compressible thin-layer Navier-Stokes equations. The authors reported computa-

tional times of about five minutes per airfoil, and about 56 hours for the total optimization process, using a NEC SX-6 computing system with 32 processors. Eighteen robust nondominated solutions were obtained in the first test case. From this set, almost half of the population attained the  $6\sigma$  condition. In the second test case, more robust nondominated solutions were found, and they satisfied a sigma level as high as  $25\sigma$ .

- Lee et al. [24] presented the robust design optimization of an ONERA M6 Wing Shape. The robust optimization was based on the concept of the Taguchi method in which the optimization problem is solved considering uncertainties in the design environment, in this case, the flow Mach number. The problem had two objectives: (i) minimization of the mean value of an objective function with respect to variability of the operating conditions, and (ii) minimization of the variance of the objective function of each candidate solution, with respect to its mean value. In the sample problems, the wing was defined by means of its planform shape (sweep angle, aspect ratio, taper ratio, etc.) and of the airfoil geometry, at three wing locations (each airfoil shape was defined with a combination of mean lines and camber distributions), using a total of 80 design variables to define the wing designs. Geometry constraints were defined by upper and lower limits of the design variables. The authors adopted the Hierarchical Asynchronous Parallel Multi-Objective Evolutionary Algorithm (HAPMOEA) algorithm [15], which is based on evolution strategies, incorporating the concept of Covariance Matrix Adaptation (CMA). The aerodynamic evaluation was done with a CFD simulation. 12 solutions were obtained in the robust design of the wing. All the nondominated solutions showed a better behavior, in terms of aerodynamic performance (lift-to-drag ratio) with a varying Mach number, as compared to the baseline design. During the evolutionary process, a total of 1100 individuals were evaluated in approximately 100 hours of CPU time.

### 3.4.1 Comments on robust design optimization

As can be seen from the previous examples, robust solutions can be achieved in evolutionary optimization in different ways. One simple approach is to add perturbations to the design variables or environmental parameters before the fitness is evaluated, which is known as implicit averaging [50]. An alternative to implicit averaging is explicit averaging, which means that the fitness value of a given design is averaged over a number of designs generated by adding random perturbations to the original design. One drawback of the explicit averaging method is the number of additional quality evaluations needed, which can turn the approach impractical. In order to tackle this problem, metamodeling techniques have been considered [32].

### 3.5 *Multi-disciplinary design optimization*

Multi-disciplinary design optimization (MDO) aims at incorporating optimization methods to solve design problems, considering not only one engineering discipline, but a set of them. The optimum of a multidisciplinary problem might be a compromise solution from the multiple disciplines involved. In this sense, multi-objective optimization is well suited for this type of problems, since it can exploit the interactions between the disciplines, and can help to find the trade-offs among them. Next, we present some work in which MOEAs have been used for aerodynamic shape optimization problems, coupled with another discipline.

- Chiba et al. [8] addressed the MDO problem of a wing shape for a transonic regional-jet aircraft. In this case, three objective functions were minimized: (i) block fuel for a required airplane's mission, (ii) maximum take-off weight, and (iii) difference in the drag coefficient between transonic and subsonic flight conditions. Additionally, five constraints were imposed, three of which were related to the wing's geometry and two more to the operating conditions in lift coefficient and to the fuel volume required for a predefined aircraft mission. The wing geometry was defined by 35 design variables. The authors adopted ARMOGA [40]. The disciplines involved included aerodynamics and structural analysis and during the optimization process, an iterative aeroelastic solution was generated in order to minimize the wing weight, with constraints on flutter and strength requirements. Also, a flight envelope analysis was done, obtaining high-fidelity Navier-Stokes solutions for various flight conditions. Although the authors used very small population sizes (eight individuals), about 880 hours of CPU time were required at each generation, since an iterative process was performed in order to optimize the wing weight, subject to aeroelastic and strength constraints. The population was reinitialized at every 5 generations for range adaptation of the design variables. In spite of the use of such a reduced population size, the authors were able to find several nondominated solutions outperforming the initial design. They also noted that during the evolution, the wing-box weight tended to increase, but this degrading effect was redeemed by an increase in aerodynamic efficiency, given a reduction in the block fuel of over one percent, which would be translated in significant savings for an airline's operational costs.
- Sasaki et al. [41] used MDO for the design of a supersonic wing shape. In this case, four objective functions were minimized: (i) drag coefficient at transonic cruise, (ii) drag coefficient at supersonic cruise, (iii) bending moment at the wing root at supersonic cruise condition, and (iv) pitching moment at supersonic cruise condition. The problem was defined by 72 design variables. Constraints were imposed on the variables ranges and on the wing section's thickness and camber, all of them being geometrical constraints. The authors adopted ARMOGA [40], and the aerodynamic evaluation of the design solutions, was done by high-fidelity Navier-Stokes CFD simulations. No aeroelastic analysis was performed, which considerably reduced the total computational cost. The objective associated with the bending moment at wing root was evaluated by numerical integration of the

pressure distribution over the wing surface, as obtained by the CFD analysis. The authors indicated that among the nondominated solutions there were designs that were better in all four objectives with respect to a reference design.

- Lee et al. [23] utilized a generic Framework for MDO to explore the improvement of aerodynamic and radar cross section (RCS) characteristics of an Unmanned Combat Aerial Vehicle (UCAV). In this application, two disciplines were considered, the first concerning the aerodynamic efficiency, and the second related to the visual and radar signature of an UCAV airplane. In this case, three objective functions were minimized: (i) inverse of the lift/drag ratio at ingress condition, (ii) inverse of the lift/drag ratio at cruise condition, and (iii) frontal area. The number of design variables was of approximately 100 and only side constraints were considered in the design variables. The first two objective functions were evaluated using a Potential Flow CFD Solver (FLO22) [17] coupled to FRICTION code to obtain the viscous drag, using semi-empirical relations. The authors adopted the Hierarchical Asynchronous Parallel Multi-Objective Evolutionary Algorithm (HAPMOEA) [15]. The authors reported a processing time of 200 hours for their approach, on a single 1.8 GHz processor. It is important to consider that HAPMOEA operates with different CFD grid levels (i.e. approximation levels): coarse, medium, and fine. In this case, the authors adopted different population sizes for each of these levels. Also, solutions were allowed to migrate from a low/high fidelity level to a higher/lower one in an island-like mechanism.

### 3.5.1 Comments on multidisciplinary design optimization

The increasing complexity of engineering systems has raised the interest in multidisciplinary optimization, as can be seen from the examples presented in this section. For this task, MOEAs facilitate the integration of several disciplines, since they do not require additional information other than the evaluation of the corresponding objective functions, which is usually done by each discipline and by the use of simulations. Additionally, an advantage of the use of MOEAs for MDO, is that they can easily manage any combination of variable types, coming from the involved disciplines i.e., from the aerodynamic discipline, the variables can be continuous, but for the structural optimization, it can happen that the variables are discrete. Kuhn et al. [22] presented an example of this condition for the multi-disciplinary design of an airship. However, one challenge in MDO is the increasing dimensionality attained in the design space, as the number of disciplines also increases.

## 3.6 Data mining and knowledge extraction

Data mining tools, along with data visualization using graphical methods, can help to understand and extract information from the data contained in the Pareto opti-



mal solutions found using any MOEA. In this sense, Multi-Objective Design Exploration (MODE), proposed by Jeong et al. [18] is a framework to extract design knowledge from the obtained Pareto optimal solutions such as trade-off information between contradicting objectives and sensitivity of each design parameter to the objectives. In the framework of MODE, Pareto-optimal solutions are obtained by a MOEA and knowledge is extracted by analyzing the design parameter values and the objective function values of the obtained Pareto-optimal solutions using data mining approaches such as Self Organizing Maps (SOMs) and analysis of variance (ANOVA). They also propose to use rough sets theory to obtain rules from the Pareto optimal solutions. MODE has been applied to a wide variety of design optimization problems as summarized next:

- Jeong et al. [18] and Chiba et al. [7, 6] explored the trade-offs among four aerodynamic objective functions in the optimization of a wing shape for a Reusable Launch Vehicle (RLV). The objective functions were: (i) The shift of the aerodynamic center between supersonic and transonic flight conditions, (ii) Pitching moment in the transonic flight condition, (iii) drag in the transonic flight condition, and (iv) lift for the subsonic flight condition. The first three objectives were minimized while the fourth was maximized. These objectives were selected for attaining control, stability, range and take-off constraints, respectively. The RLV definition comprised 71 design variables to define the wing planform, the wing position along the fuselage and the airfoil shape at prescribed wingspan stations. The authors adopted ARMOGA [40], and the aerodynamic evaluation of the RLV was done with a Reynolds-Averaged Navier-Stokes CFD simulation. A trade-off analysis was conducted with 102 nondominated individuals generated by the MOEA. Data mining with SOM was used, and some knowledge was extracted in regards to the correlation of each design variable to the objective functions in [7]; with SOM, Batch-SOM, ANOVA and rough sets in [6]; and with SOM, Batch-SOM and ANOVA in [18]. In all cases, some knowledge was extracted in regards to the correlation of each design variable to the objective functions.
- Oyama et al. [35] applied a design exploration technique to extract knowledge information from a flapping wing MAV (Micro Air Vehicle). The flapping motion of the MAV was analyzed using multi-objective design optimization techniques in order to obtain nondominated solutions. Such nondominated solutions were further analyzed with SOMs in order to extract knowledge about the effects of the flapping motion parameters on the objective functions. The conflicting objectives considered were: (i) maximization of the time-averaged lift coefficient, (ii) maximization of the time-averaged thrust coefficient, and (iii) minimization of the time-averaged required power coefficient. The problem had five design variables and the geometry of the flying wing was kept fixed. Constraints were imposed on the averaged lift and thrust coefficients so that they were positive. The authors adopted a GA-based MOEA. The objective functions were obtained by means of CFD simulations, solving the unsteady incompressible Navier-Stokes equations. Objective functions were averaged over one flapping cycle. The purpose of the study was to extract trade-off information from the objective functions and the

flapping motion parameters such as plunge amplitude and frequency, pitching angle amplitude and offset.

- Tani et al. [49] solved a multiobjective rocket engine turbopump blade shape optimization design which considered three objective functions: (i) shaft power, (ii) entropy rise within the stage, and (iii) angle of attack of the next stage. The first objective was maximized while the others were minimized. The design candidates defined the turbine blade aerodynamic shape and consisted of 58 design variables. The authors adopted MOGA [14] as their search engine. The objective function values were obtained from a CFD Navier-Stokes flow simulation. The authors reported using SOMs to extract correlation information for the design variables with respect to each objective function.

### 3.6.1 Comments on data mining and knowledge extraction

When adopting the data mining techniques used in the above examples, in which analyses are done, correlating the objective functions values, with the design parameter values of the Pareto optimal solutions, some valuable information is obtained. However, in many other cases, for aerodynamic flows, the knowledge required is more related to the physics, rather than to the geometry, given by the design variables. For example, for understanding the relation between the generation of shock wave formation and aerodynamic characteristics in a transonic airfoil optimization. For this, Oyama et al. [34], have recently proposed a new approach to extract useful design information from one-dimensional, two-dimensional, and three-dimensional flow data of Pareto-optimal solutions. They use a flow data analysis by Proper Orthogonal Decomposition (POD), which is a statistical approach that can extract dominant features in the data by decomposing it into a set of optimal orthogonal base vectors of decreasing importance.

## 4 A Case Study

Here, we present a case study of evolutionary multi-objective optimization for an airfoil shape optimization problem. The test problem chosen corresponds to the airfoil shape of a standard-class glider. The optimization problem aims at obtaining optimum performance for a sailplane. In this study the trade-off among three aerodynamic objectives is evaluated using a MOEA.

### 4.1 Objective functions

Three conflicting objective functions are defined in terms of a sailplane average weight and operating conditions [48]. They are formally defined as:



- (i) Minimize  $C_D/C_L$  subject to  $C_L = 0.63$ ,  $Re = 2.04 \cdot 10^6$ ,  $M = 0.12$
- (ii) Minimize  $C_D/C_L$  subject to  $C_L = 0.86$ ,  $Re = 1.63 \cdot 10^6$ ,  $M = 0.10$
- (iii) Minimize  $C_D/C_L^{3/2}$  subject to  $C_L = 1.05$ ,  $Re = 1.29 \cdot 10^6$ ,  $M = 0.08$

In the above definitions,  $C_D/C_L$  and  $C_D/C_L^{3/2}$  correspond to the inverse of the glider's gliding ratio and sink rate, respectively. Both are important performance measures for this aerodynamic optimization problem.  $C_D$  and  $C_L$  are the drag and lift coefficients. In the above objective function definitions, the aim is to maximize the gliding ratio for objectives (i) and (ii), while minimizing the sink rate in objective (iii). Each of these objectives is evaluated at different prescribed flight conditions, given in terms of Mach and Reynolds numbers.

## 4.2 Geometry parameterization

Finding an optimum representation scheme for aerodynamic shape optimization problems is an important step for a successful aerodynamic optimization task. Several options can be used for airfoil shape parameterization.

- (a) The representation used needs to be flexible to describe any general airfoil shape.
- (b) The representation also needs to be efficient, in order that the parameterization can be achieved with a minimum number of parameters. Inefficient representations may result in an unnecessarily large design space which, in consequence, can reduce the search efficiency of an evolutionary algorithm.
- (c) The representation should allow the use of any optimization algorithm to perform local search. This requirement is important for refining the solutions obtained by the global search engine in a more efficient way.

In the present case study, the PARSEC airfoil representation [45] is used. Fig. 1 illustrates the 11 basic parameters used for this representation:  $r_{le}$  leading edge radius,  $X_{up}/X_{lo}$  location of maximum thickness for upper/lower surfaces,  $Z_{up}/Z_{lo}$  maximum thickness for upper/lower surfaces,  $Z_{xxup}/Z_{xxlo}$  curvature for upper/lower surfaces, at maximum thickness locations,  $Z_{te}$  trailing edge coordinate,  $\Delta Z_{te}$  trailing edge thickness,  $\alpha_{te}$  trailing edge direction, and  $\beta_{te}$  trailing edge wedge angle. For the present case study, the modified PARSEC geometry representation adopted allows us to define independently the leading edge radius, both for upper and lower surfaces. Thus, 12 variables in total are used. Their allowable ranges are defined in Table 1.

The PARSEC airfoil geometry representation uses a linear combination of shape functions for defining the upper and lower surfaces. These linear combinations are given by:

	$r_{leup}$	$r_{lelo}$	$\alpha_{te}$	$\beta_{te}$	$Z_{te}$	$\Delta Z_{te}$	$X_{up}$	$Z_{up}$	$Z_{xxup}$	$X_{lo}$	$Z_{lo}$	$Z_{xxlo}$
min	0.0085	0.002	7.0	10.0	-0.006	0.0025	0.41	0.11	-0.9	0.20	-0.023	0.05
max	0.0126	0.004	10.0	14.0	-0.003	0.0050	0.46	0.13	-0.7	0.26	-0.015	0.20

**Table 1** Parameter ranges for modified PARSEC airfoil representation

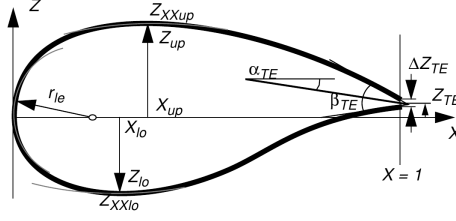


**Fig. 1** PARSEC airfoil parameterization

$$Z_{upper} = \sum_{n=1}^6 a_n x^{\frac{n-1}{2}} \quad (4)$$

$$Z_{lower} = \sum_{n=1}^6 b_n x^{\frac{n-1}{2}} \quad (5)$$

In the above equations, the coefficients  $a_n$ , and  $b_n$  are determined as function of the 12 described geometric parameters, by solving the following two systems of linear equations:

*Upper surface:*

$$\begin{bmatrix} 1 & 1 & 1 & 1 & 1 & 1 \\ X_{up}^{1/2} & X_{up}^{3/2} & X_{up}^{5/2} & X_{up}^{7/2} & X_{up}^{9/2} & X_{up}^{11/2} \\ 1/2 & 3/2 & 5/2 & 7/2 & 9/2 & 11/2 \\ \frac{1}{2}X_{up}^{-1/2} & \frac{3}{2}X_{up}^{1/2} & \frac{5}{2}X_{up}^{3/2} & \frac{7}{2}X_{up}^{5/2} & \frac{9}{2}X_{up}^{7/2} & \frac{11}{2}X_{up}^{9/2} \\ -\frac{1}{4}X_{up}^{-3/2} & \frac{3}{4}X_{up}^{-1/2} & \frac{15}{4}X_{up}^{1/2} & \frac{35}{4}X_{up}^{3/2} & \frac{63}{4}X_{up}^{5/2} & \frac{99}{4}X_{up}^{7/2} \\ 1 & 0 & 0 & 0 & 0 & 0 \end{bmatrix} \begin{bmatrix} a_1 \\ a_2 \\ a_3 \\ a_4 \\ a_5 \\ a_6 \end{bmatrix} = \begin{bmatrix} Z_{te} + \frac{1}{2}\Delta Z_{te} \\ Z_{up} \\ \tan((2\alpha_{te} - \beta_{te})/2) \\ 0 \\ Z_{xxup} \\ \sqrt{r_{leup}} \end{bmatrix} \quad (6)$$

It is important to note that the geometric parameters  $r_{leup}/r_{lelo}$ ,  $X_{up}/X_{lo}$ ,  $Z_{up}/Z_{lo}$ ,  $Z_{xxup}/Z_{xxlo}$ ,  $Z_{te}$ ,  $\Delta Z_{te}$ ,  $\alpha_{te}$ , and  $\beta_{te}$  are the actual design variables in the optimization process, and that the coefficients  $a_n$ ,  $b_n$  serve as intermediate variables for interpolating the airfoil's coordinates, which are used by the CFD solver (we used the Xfoil CFD code [13]) for its discretization process.

*Lower surface:*

$$\begin{bmatrix} 1 & 1 & 1 & 1 & 1 & 1 \\ X_{lo}^{1/2} & X_{lo}^{3/2} & X_{lo}^{5/2} & X_{lo}^{7/2} & X_{lo}^{9/2} & X_{lo}^{11/2} \\ 1/2 & 3/2 & 5/2 & 7/2 & 9/2 & 11/2 \\ \frac{1}{2}X_{lo}^{-1/2} & \frac{3}{2}X_{lo}^{1/2} & \frac{5}{2}X_{lo}^{3/2} & \frac{7}{2}X_{lo}^{5/2} & \frac{9}{2}X_{lo}^{7/2} & \frac{11}{2}X_{lo}^{9/2} \\ -\frac{1}{4}X_{lo}^{-3/2} & \frac{3}{4}X_{lo}^{-1/2} & \frac{15}{4}X_{lo}^{1/2} & \frac{35}{4}X_{lo}^{3/2} & \frac{63}{4}X_{lo}^{5/2} & \frac{99}{4}X_{lo}^{7/2} \\ 1 & 0 & 0 & 0 & 0 & 0 \end{bmatrix} \begin{bmatrix} b_1 \\ b_2 \\ b_3 \\ b_4 \\ b_5 \\ b_6 \end{bmatrix} = \begin{bmatrix} Z_{te} - \frac{1}{2}\Delta Z_{te} \\ Z_{lo} \\ \tan((2\alpha_{te} + \beta_{te})/2) \\ 0 \\ Z_{xto} \\ -\sqrt{r_{lelo}} \end{bmatrix} \quad (7)$$

### 4.3 Constraints

For this case study, five constraints are considered. The first three are defined in terms of flight speed for each objective function, namely the prescribed  $C_L$  values,  $C_L = 0.63$  for objective (i),  $C_L = 0.86$  for objective (ii), and  $C_L = 1.05$  for objective (iii), enable the glider to fly at a given design speed, and to produce the necessary amount of lift to balance the gravity force for each design condition being analyzed. It is important to note that prescribing the required  $C_L$ , the corresponding angle of attack  $\alpha$  for the airfoil is obtained as an additional variable. For this, the flow solver, given the design candidate geometry, solves the flow equations with a constraint on the  $C_L$  value, i.e., it additionally determines the operating angle of attack  $\alpha$ . Two additional constraints are defined for the airfoil geometry. First, the maximum airfoil thickness range is defined by  $13.0\% \leq t/c \leq 13.5\%$ . For handling this constraint, every time a new design candidate is created by the evolutionary operators, its maximum thickness is checked and corrected before being evaluated. The correction is done by scaling accordingly the design parameters  $Z_{up}$  and  $Z_{lo}$ , which mainly define the thickness distribution in the airfoil. In this way, only feasible solutions are evaluated by the simulation process. The final constraint is the trailing edge thickness, whose range is defined by  $0.25\% \leq \Delta Z_{te} \leq 0.5\%$ . This constraint is directly handled in the lower and upper bounds by the corresponding  $\Delta Z_{te}$  design parameter.

### 4.4 Evolutionary algorithm

For solving the above case study, we adopted MODE-LD+SS [3] as our search algorithm. Additionally, and for comparison purposes, we also used an implementation of the SMS-EMOA algorithm [5]. This algorithm is based on the hypervolume performance measure [53] and has also been used in the context of airfoil optimization problems.

**Algorithm 1** MODE-LD+SS

---

```

1: INPUT:
    $P[1, \dots, N]$  = Population
    $N$  = Population Size
    $F$  = Scaling factor
    $CR$  = Crossover Rate
    $\lambda[1, \dots, N]$  = Weight vectors
    $NB$  = Neighborhood Size
    $GMAX$  = Maximum number of generations
2: OUTPUT:
    $PF$  = Pareto front approximation
3: Begin
4:  $g \leftarrow 0$ 
5: Randomly create  $P_i^g, i = 1, \dots, N$ 
6: Evaluate  $P_i^g, i = 1, \dots, N$ 
7: while  $g < GMAX$  do
8:    $\{LND\} = \{\emptyset\}$ 
9:   for  $i = 1$  to  $N$  do
10:     $DetermineLocalDominance(P_i^g, NB)$ 
11:    if  $P_i^g$  is locally nondominated then
12:       $\{LND\} \leftarrow \{LND\} \cup P_i^g$ 
13:    end if
14:  end for
15:  for  $i = 1$  to  $N$  do
16:    Randomly select  $\mathbf{u}_1, \mathbf{u}_2$ , and  $\mathbf{u}_3$  from  $\{LND\}$ 
17:     $\mathbf{v} \leftarrow CreateMutantVector(u_1, u_2, u_3)$ 
18:     $P_i^{g+1} \leftarrow Crossover(P_i^g, \mathbf{v})$ 
19:    Evaluate  $P_i^{g+1}$ 
20:  end for
21:   $Q \leftarrow P^g \cup P^{g+1}$ 
22:  Determine  $z^*$  for  $Q$ 
23:  for  $i = 1$  to  $N$  do
24:     $P_i^{g+1} \leftarrow MinimumTchebycheff(Q, \lambda^i, z^*)$ 
25:     $Q \leftarrow Q \setminus P_i^{g+1}$ 
26:  end for
27:   $PF \leftarrow \{P\}^{g+1}$ 
28: end while
29: Return  $PF$ 
30: End

```

---

The Multi-objective Evolutionary Algorithm MODE-LD+SS (see Algorithm 1) [3] adopts the evolutionary operators from differential evolution [36]. In the basic DE algorithm, and during the offspring creation stage, for each current vector  $P_i \in \{P\}$ , three parents (mutually different among them)  $\mathbf{u}_1, \mathbf{u}_2, \mathbf{u}_3 \in \{P\}$  ( $\mathbf{u}_1 \neq \mathbf{u}_2 \neq \mathbf{u}_3 \neq P_i$ ) are randomly selected for creating a mutant vector  $\mathbf{v}$  using the following mutation operation:

$$\mathbf{v} \leftarrow \mathbf{u}_1 + F \cdot (\mathbf{u}_2 - \mathbf{u}_3) \quad (8)$$

$F > 0$ , is a real constant *scaling factor* which controls the amplification of the difference  $(\mathbf{u}_2 - \mathbf{u}_3)$ . Using this mutant vector, a new offspring  $P'_i$  (also called trial vector in DE) is created by crossing over the mutant vector  $\mathbf{v}$  and the current solution  $P_i$ , in accordance to:

$$P'_j = \begin{cases} v_j & \text{if } (rand_j(0,1) \leq CR \text{ or } j = j_{rand}) \\ P_j & \text{otherwise} \end{cases} \quad (9)$$

In the above expression, the index  $j$  refers to the  $j$ th component of the decision variables vectors.  $CR$  is a positive constant and  $j_{rand}$  is a randomly selected integer in the range  $[1, \dots, D]$  (where  $D$  is the dimension of the solution vectors) ensuring that the offspring is different at least in one component with respect to the current solution  $P_i$ . The above DE variant is known as *Rand/1/bin*, and is the version adopted here. Additionally, the proposed algorithm incorporates two mechanisms for improving both the convergence towards the Pareto front, and the uniform distribution of nondominated solutions along the Pareto front. These mechanisms correspond to the concept of local dominance and the use of an environmental selection based on a scalar function. Below, we explain these two mechanisms in more detail.

As for the first mechanism, local dominance concept, in Algorithm 1, the solution vectors  $\mathbf{u}_1, \mathbf{u}_2, \mathbf{u}_3$ , required for creating the trial vector  $\mathbf{v}$  (in equation (8)), are selected from the current population, only if they are locally nondominated in their neighborhood  $\mathfrak{N}$ . Local dominance is defined as follows:

**Definition 6. Pareto Local Dominance** Let  $\mathbf{x}$  be a feasible solution,  $\mathfrak{N}(\mathbf{x})$  be a neighborhood structure for  $\mathbf{x}$  in the decision space, and  $\mathbf{f}(\mathbf{x})$  a vector of objective functions.

- We say that a solution  $\mathbf{x}$  is locally nondominated with respect to  $\mathfrak{N}(\mathbf{x})$  if and only if there is no  $\mathbf{x}'$  in the neighborhood of  $\mathbf{x}$  such that  $\mathbf{f}(\mathbf{x}') \prec \mathbf{f}(\mathbf{x})$

The neighborhood structure is defined as the  $NB$  closest individuals to a particular solution. Closeness is measured by using the Euclidean distance between solutions in the design variable space. The major aim of using the local dominance concept, as defined above, is to exploit good individuals' genetic information in creating DE trial vectors, and the associated offspring, which might help to improve the MOEA's convergence rate toward the Pareto front. From Algorithm 1, it can be noted that this mechanism has a stronger effect during the earlier generations, where the portion of nondominated individuals is low in the global population, and progressively weakens, as the number of nondominated individuals grows during the evolutionary process. This mechanism is automatically switched off, once all the individuals in the population become nondominated, and has the possibility of being switched on, as some individuals become dominated.

As for the second mechanism, *selection based on a scalar function*, it is based on the Tchebycheff scalarization function given by:

$$g(\mathbf{x}|\lambda, z^*) = \max_{1 \leq i \leq m} \{\lambda^i |f_i(\mathbf{x}) - z_i^*|\} \quad (10)$$

In the above equation,  $\lambda^i, i = 1, \dots, N$  represents the set of weight vectors used to distribute the solutions along the entire Pareto front. In this case, this set is calculated using the procedure described in [52].  $z^*$  corresponds to a reference point, defined in objective space and determined with the minimum objective values of the combined population  $Q$ , consistent on the actual parents and the created offspring. This reference point is updated at each generation, as the evolution progresses. The procedure *MinimumTchebycheff*( $Q, \lambda^i, z^*$ ) finds, from the set  $Q$ , (the combined population consistent on the actual parents and the created offspring), the solution vector that minimizes equation (10) for each weight vector  $\lambda^i$  and the reference point  $z^*$ .

The second MOEA adopted is the SMS-EMOA, which is a steady-state algorithm based on two basic characteristics: (1) non-dominated sorting is used as its ranking criterion and (2) the hypervolume<sup>5</sup> is applied as its selection criterion to discard that individual, which contributes the least hypervolume to the worst-ranked front.

The basic algorithm is described in Algorithm 2. Starting with an initial population of  $\mu$  individuals, a new individual is generated by means of randomised variation operators. We adopted simulated binary crossover (SBX) and polynomial-based mutation as described in [11]. The new individual will become a member of the next population, if replacing another individual leads to a higher quality of the population with respect to the hypervolume.

---

#### Algorithm 2 SMS-EMOA

---

```

1:  $P_0 \leftarrow \text{init}()$  /* initialize random population of  $\mu$  individuals */
2:  $t \leftarrow 0$ 
3: repeat
4:    $q_{t+1} \leftarrow \text{generate}(P_t)$  /* generate offspring by variation */
5:    $P_{t+1} \leftarrow \text{reduce}(P_t \cup \{q_{t+1}\})$  /* select  $\mu$  best individuals */
6: until termination condition is fulfilled

```

---

The procedure **Reduce** described in Algorithm 2 selects the  $\mu$  individuals of the subsequent population. The algorithm fast-nondominated-sort used in NSGA-II [12] is applied to partition the population into  $v$  sets  $\mathcal{R}_1, \dots, \mathcal{R}_v$ . The subsets are called fronts and are provided with an index representing a hierarchical order (the level of domination) whereas the solutions within each front are mutually nondominated. The first subset contains all nondominated solutions of the original set  $Q$ . The second front consists of individuals that are nondominated in the set  $(Q \setminus \mathcal{R}_1)$ , e.g. each member of  $\mathcal{R}_2$  is dominated by at least one member of  $\mathcal{R}_1$ . More general, the  $i$ th front consists of individuals that are nondominated if the individuals of the fronts  $j$  with  $j < i$  were removed from  $Q$ .

The value of  $\Delta_{\mathcal{S}}(s, \mathcal{R}_v)$  can be interpreted as the exclusive contribution of  $s$  to the hypervolume value of its appropriate front. By definition of  $\Delta_{\mathcal{S}}(s, \mathcal{R}_v)$ , an individual, which dominates another is always kept and a nondominated individual is replaced by a dominated one. This measure keeps those individuals which maxi-

---

<sup>5</sup> The **Hypervolume** (also known as the  $S$ -metric or the Lebesgue Measure) of a set of solutions measures the size of the portion of objective space that is dominated by those solutions collectively.

**Algorithm 3 Reduce( $Q$ )**


---

```

1:  $\{\mathcal{R}_1, \dots, \mathcal{R}_v\} \leftarrow \text{fast\_nondominated\_sort}(Q)$  /* all  $v$  fronts of  $Q^*$ /
2:  $r \leftarrow \text{argmin}_{s \in \mathcal{R}_v} [\Delta_{\mathcal{S}}(s, \mathcal{R}_v)]$  /*  $s \in \mathcal{R}_v$  with lowest  $\Delta_{\mathcal{S}}(s, \mathcal{R}_v)^*$ /
3: return  $(Q \setminus r)$ 

```

---

mize the population's S-Metric value, which implies that the covered hypervolume of a population cannot decrease by application of the **Reduce** operator. Thus, for Algorithm 1 the following invariant holds:

$$\mathcal{S}(P_t) \leq \mathcal{S}(P_{t+1}) \quad (11)$$

Due to the high computational effort of the hypervolume calculation, a steady state selection scheme is used. Since only one individual is created, only one has to be deleted from the population at each generation. Thus, the selection operator has to compute at most  $\mu + 1$  values of the S-Metric (exactly  $\mu + 1$  values in case all solutions are nondominated). These are the values of the subsets of the worst ranked front, in which one point of the front is left out, respectively. A  $(\mu + \lambda)$  selection scheme would require the calculation of  $\binom{\mu + \lambda}{\mu}$  possible S-Metric values to identify an optimally composed population, maximising the S-Metric net value.

The parameters used for solving the present case study, and for each algorithm were set as follows:  $N = 120$  (population size) for both MOEAs,  $F = 0.5$  (mutation scaling factor for MODE-LD+SS),  $CR = 0.5$  (crossover rate for MODE-LD+SS),  $NB = 5$  (neighborhood size for MODE-LD+SS),  $\eta_m = 20$  (mutation index for SBX in SMS-EMOA), and  $\eta_c = 15$  (crossover index for SBX in SMS-EMOA).

## 4.5 Results

Both, MODE-LD+SS and SMS-EMOA were run for 100 generations. The simulation process in each case took approximately 8 hrs of CPU time. Five independent runs were executed for extracting some statistics. Figs. 2 to 3 show the Pareto front approximations (of the median run) at different evolution times. For comparison purposes, in these figures the corresponding objective functions of a reference airfoil (a720o [48]) are plotted. At  $t = 10$  generations (the corresponding figure is not shown due to space constraints), the number of nondominated solutions is 26 for SMS-EMOA and 27 for MODE-LD+SS. With this small number of nondominated solutions is difficult to identify the trade-off surface for this problem. However, as the number of evolution steps increases, the trade-off surface is more clearly revealed. At  $t = 50$  generations (see Fig. 2), the number of nondominated solutions is 120 for SMS-EMOA, and 91 for MODE-LD+SS. At this point, the trade-off surface shows a steeper variation of objective (iii) toward the compromise region of the Pareto front. Also, the trade-off shows a plateau where the third objective has a small variation with respect to the other objectives. Finally, at  $t = 100$  generations

(see Fig. 3), the shape of the trade-off surface is more clearly defined, and a clear trade-off between the three objectives are evidenced. It is important to note in Fig. 3, that the trade-off surface shows some void regions. This condition is captured by both MOEAs and is attributed to the constraints defined in the airfoil geometry. Table 2 summarizes the maximum possible improvement with respect to the reference solution, that can be attained for each objective and by each MOEA.

	MOEA					
	SMS-EMOA			MODE-LD+SS		
Gen	$\Delta Obj1(\%)$	$\Delta Obj2(\%)$	$\Delta Obj3(\%)$	$\Delta Obj1(\%)$	$\Delta Obj2(\%)$	$\Delta Obj3(\%)$
10	11.43	10.19	5.43	11.93	10.38	5.47
50	12.84	10.67	6.06	13.22	10.67	6.21
100	12.75	10.79	6.28	13.63	10.80	6.40

**Table 2** Maximum improvement per objective for the median run of each MOEA used

In the context of MOEAs, it is common to compare results on the basis of some performance measures. Next, and for comparison purposes between the algorithms used, we present the hypervolume values attained by each MOEA, as well as the values of the two set coverage performance measure C-M(A,B) between them. Next, we present the definition for these two performance measures:

**Hypervolume (Hv):** Given a Pareto approximation set  $PF_{known}$ , and a reference point in objective space  $z_{ref}$ , this performance measure estimates the *Hypervolume* attained by it. Such hypervolume corresponds to the non-overlapping volume of all the hypercubes formed by the reference point ( $z_{ref}$ ) and every vector in the Pareto set approximation. This is mathematically defined as:

$$HV = \{\cup_i vol_i | vec_i \in PF_{known}\} \quad (12)$$

$vec_i$  is a nondominated vector from the Pareto set approximation, and  $vol_i$  is the volume for the hypercube formed by the reference point and the nondominated vector  $vec_i$ . Here, the reference point ( $z_{ref}$ ) in objective space for the 3-objective MOPs was set to (0.007610 , 0.005895 , 0.005236 ), which corresponds to the objective values of the reference airfoil. High values of this measure indicate that the solutions are closer to the true Pareto front and that they cover a wider extension of it.

**Two Set Coverage (C-Metric):** This performance measure estimates the coverage proportion, in terms of percentage of dominated solutions, between two sets. Given the sets  $A$  and  $B$ , both containing only nondominated solutions, the C-Metric is mathematically defined as:

$$C(A,B) = \frac{|\{u \in B | \exists v \in A : v \text{ dominates } u\}|}{|B|} \quad (13)$$



This performance measure indicates the portion of vectors in  $B$  being dominated by any vector in  $A$ . The sets  $A$  and  $B$  correspond to two different Pareto approximations, as obtained by two different algorithms. Therefore, the C-Metric is used for pairwise comparisons between algorithms.

For the hypervolume measure, SMS-EMOA attains a value of  $H_v = 1.5617 \cdot 10^{-10}$  with a standard deviation of  $\sigma = 2.4526 \cdot 10^{-12}$ , while MODE-LD+SS attains a value of  $H_v = 1.6043 \cdot 10^{-10}$  with a standard deviation of  $\sigma = 1.2809 \cdot 10^{-12}$ . These results are the average of five independent runs executed by each algorithm.

As for the C-Metric, the corresponding values obtained are:  $C - M(SMS - EMOA, MODE - LD + SS) = 0.07016$  with a standard deviation of  $\sigma = 0.03134$ , and  $C - M(MODE - LD + SS, SMS - EMOA) = 0.3533$  with a standard deviation of  $\sigma = 0.0510$ . These latter results are the average of all the pairwise combinations of the five independent runs executed by each algorithm. Our results indicate that MODE-LD+SS converges closer to the true Pareto front, and provides more non-dominated solutions than SMS-EMOA.

Finally, in Figure 4 are presented the geometries of the reference airfoil, a720o, and two selected airfoils from the trade-off surface of this problem and obtained by SMS-EMOA and MODE-LD+SS at  $t = 100$  generations. These two latter airfoil are selected as those with the closest distance to the origin of the objective space, since they are considered to represent the best trade-off solutions.

## 5 Conclusions and final remarks

In this chapter we have presented a brief review of the research done on multi-objective aerodynamic shape optimization. The examples presented cover a wide range of current applications of these techniques in the context of aeronautical engineering design, and in several design scenarios. The approaches reviewed include the use of surrogates, hybridizations with gradient-based techniques, mechanisms to search for robust solutions, multidisciplinary approaches, and knowledge extraction techniques. It can be observed that several Pareto-based MOEAs have been successfully integrated in industrial problems. It can be anticipated that in the near future, an extended use of these techniques will be a standard practice, as the computing power available continues to increase each year. It is also worth noting that MOEAs are flexible enough as to allow their coupling to both engineering models and low-order physics-based models without major changes. They can also be easily parallelized, since MOEAs normally have low data dependency.

From an algorithmic point of view, it is clear that the use of Pareto-based MOEAs remains as a popular choice in the previous group of applications. It is also evident that, when dealing with expensive objective functions such as those of the above applications, the use of careful statistical analysis of parameters is unaffordable. Thus, the parameters of such MOEAs were simple guesses or taken from values suggested by other researchers. The use of surrogate models also appears in these costly ap-

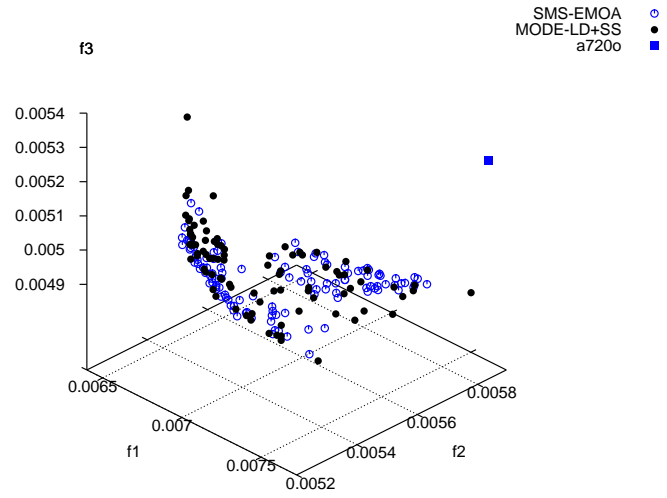


**Fig. 2** Pareto front approximation at Gen = 50 (6000 OFEs)

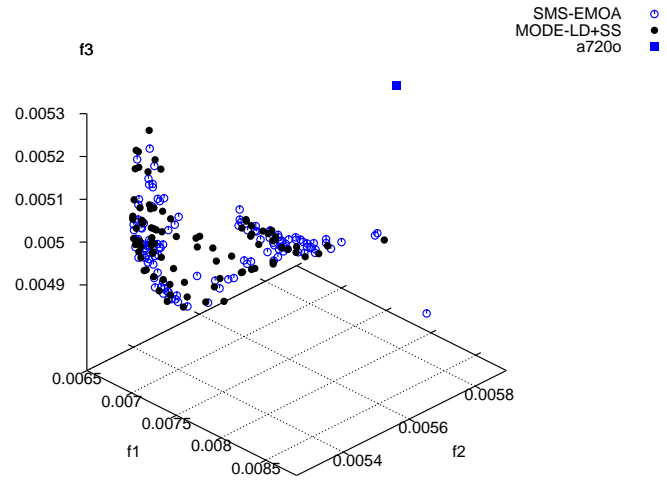


**Fig. 3** Pareto front approximation at Gen = 100 (12000 OFEs)

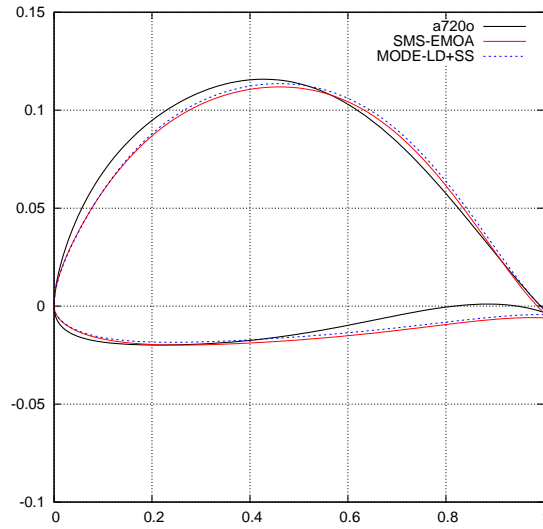


**Fig. 4** Airfoil shape comparison

plications. However, the use of other simpler techniques such as fitness inheritance or fitness approximation [39] seems to be uncommon in this domain and could be a good alternative when dealing with high-dimensional problems. Additionally, the authors of this group of applications have relied on very simple constraint-handling techniques, most of which discard infeasible individuals. Alternative approaches exist, which can exploit information from infeasible solutions and can make a more sophisticated exploration of the search space when dealing with constrained problems (see for example [29]) and this has not been properly studied yet. Finally, it is worth emphasizing that, in spite of the difficulty of these problems and of the evident limitations of MOEAs to deal with them, most authors report finding improved designs when using MOEAs, even when in all cases a fairly small number of fitness function evaluations was allowed. This clearly illustrates the high potential of MOEAs in this domain.

## Acknowledgements

The first author acknowledges support from both CONACyT and IPN to pursue graduate studies in computer science at CINVESTAV-IPN. The second author acknowledges support from CONACyT project no. 103570. The third author acknowledges support from CONACyT project no. 79809.

## References

1. Murray B. Anderson. Genetic Algorithms In Aerospace Design: Substantial Progress, Tremendous Potential. Technical report, Sverdrup Technology Inc./TEAS Group, 260 Eglin Air Force Base, FL 32542, USA, 2002.
2. Mohammad Arabnia and Wahid Ghaly. A Strategy for Multi-Objective Shape optimization of Turbine Stages in Three-Dimensional Flow. In *12th AIAA/ISSMO Multidisciplinary Analysis and Optimization Conference*, Victoria, British Columbia Canada, 10–12 September 2008.
3. Alfredo Arias Montaño, Carlos A. Coello Coello, and Efrén Mezura-Montes. MODE-LD+SS: A Novel Differential Evolution Algorithm Incorporating Local Dominance and Scalar Selection Mechanisms for Multi-Objective Optimization. In *2010 IEEE Congress on Evolutionary Computation (CEC'2010)*, Barcelona, Spain, July 2010. IEEE Press.
4. Ernesto Benini. Three-Dimensional Multi-Objective Design optimization of a Transonic Compressor Rotor. *Journal of Propulsion and Power*, 20(3):559–565, May–June 2004.
5. Nicola Beume, Boris Naujoks, and Michael Emmerich. SMS-EMOA: Multiobjective Selection Based on Dominated Hypervolume. *European Journal of Operational Research*, 181:1653–1659, 2007.
6. Kazuhisa Chiba, Shinkyu Jeong, Shigeru Obayashi, and Kazuomi Yamamoto. Knowledge Discovery in Aerodynamic Design Space for Flyback–Booster Wing Using Data Mining. In *14th AIAA/AHI Space Planes and Hypersonic System and Technologies Conference*, Canberra, Australia, November 6–9 2006.
7. Kazuhisa Chiba, Shigeru Obayashi, and Kazuhiro Nakahashi. Design Exploration of Aerodynamic Wing Shape for Reusable Launch Vehicle Flyback Booster. *Journal of Aircraft*, 43(3):832–836, May–June 2006.
8. Kazuhisa Chiba, Akira Oyama, Shigeru Obayashi, Kazuhiro Nakahashi, and Hiroyuki Morino. Multidisciplinary Design Optimization and Data Mining for Transonic Regional-Jet Wing. *AIAA Journal of Aircraft*, 44(4):1100–1112, July–August 2007. DOI: 10.2514/1.17549.
9. Hyoungh-Seog Chung, Seongim Choi, and Juan J. Alonso. Supersonic Business Jet Design using a Knowledge-Based Genetic Algorithm with an Adaptive, Unstructured Grid Methodology. In *AIAA Paper 2003-3791, 21st Applied Aerodynamics Conference*, Orlando, Florida, USA, 23–26 June 2003.
10. Carlos A. Coello Coello. Theoretical and Numerical Constraint Handling Techniques used with Evolutionary Algorithms: A Survey of the State of the Art. *Computer Methods in Applied Mechanics and Engineering*, 191(11–12):1245–1287, January 2002.
11. Kalyanmoy Deb. *Multi-Objective Optimization using Evolutionary Algorithms*. John Wiley & Sons, Chichester, UK, 2001. ISBN 0-471-87339-X.
12. Kalyanmoy Deb, Amrit Pratap, Sameer Agarwal, and T. Meyarivan. A Fast and Elitist Multiobjective Genetic Algorithm: NSGA–II. *IEEE Transactions on Evolutionary Computation*, 6(2):182–197, April 2002.
13. Mark Drela. XFOIL: An Analysis and Design System for Low Reynolds Number Aerodynamics. In *Conference on Low Reynolds Number Aerodynamics*, University Of Notre Dame, IN, June 1989.
14. Carlos M. Fonseca and Peter J. Fleming. Genetic Algorithms for Multiobjective Optimization: Formulation, Discussion and Generalization. In Stephanie Forrest, editor, *Proceedings of the Fifth International Conference on Genetic Algorithms*, pages 416–423, San Mateo, California, 1993. University of Illinois at Urbana-Champaign, Morgan Kaufman Publishers.
15. Luis F. Gonzalez. *Robust Evolutionary Methods for Multi-objective and Multidisciplinary Design Optimization in Aeronautics*. PhD thesis, School of Aerospace, Mechanical and Mechatronic Engineering, The University of Sydney, Australia, 2005.
16. Jun Hua, Fanmei Kong, Po yang Liu, and David Zingg. Optimization of Long-Endurance Airfoils. In *AIAA-2003-3500, 21st AIAA Applied Aerodynamics Conference*, Orlando, FL, June 23–26 2003.
17. A. Jameson, D.A. Caughey, P.A. Newman, and R.M. Davis. NYU Transonic Swept-Wing Computer Program - FLO22. Technical report, Langley Research Center, 1975.

18. Shinkyu Jeong, Kazuhisa Chiba, and Shigeru Obayashi. Data Mining for Aerodynamic Design Space. In *AIAA Paper 2005-5079, 23rd AIAA Applied Aerodynamic Conference*, Toronto, Ontario Canada, June 6-9 2005.
19. Yaochu Jin. A comprehensive survey of fitness approximation in evolutionary computation. *Soft Computing*, 9(1):3-12, 2005.
20. Ilan Kroo. Multidisciplinary Optimization Applications in Preliminary Design – Status and Directions. In *38th, and AIAA/ASME/AHS Adaptive Structures Forum*, Kissimmee, FL, Apr. 7-10 1997.
21. Ilan Kroo. Innovations in Aeronautics. In *42nd AIAA Aerospace Sciences Meeting*, Reno, NV, January 5-8 2004.
22. T. Kuhn, C. Rösler, and H. Baier. Multidisciplinary Design Methods for the Hybrid Universal Ground Observing Airship (HUGO). In *AIAA Paper 2007-7781*, Belfast, Northern Ireland, 18-20 September 2007.
23. D. S. Lee, L. F. Gonzalez, K. Srinivas, D. J. Auld, and K. C. Wong. Aerodynamics/RCS Shape Optimisation of Unmanned Aerial Vehicles using Hierarchical Asynchronous Parallel Evolutionary Algorithms. In *AIAA Paper 2006-3331, 24th AIAA Applied Aerodynamics Conference*, San Francisco, California, USA, June 5-8 2006.
24. D.S. Lee, L.F. Gonzalez, J. Periaux, and K. Srinivas. Robust Design Optimisation Using Multi-Objective Evolutionary Algorithms. *Computer & Fluids*, 37:565-583, 2008.
25. Leifur Leifsson and Slawomir Koziel. Multi-fidelity design optimization of transonic airfoils using physics-based surrogate modeling and shape-preserving response prediction. *Journal of Computational Science*, pages 98-106, 2010.
26. Yongsheng Lian and Meng-Sing liou. Multiobjective Optimization Using Coupled Response Surface Model and Evolutionary Algorithm. In *AIAA Paper 2004-4323, 10th AIAA/ISSMO Multidisciplinary Analysis and Optimization Conference*, Albany, New York, USA, 30 August-1 September 2004.
27. Yongsheng Lian and Meng-Sing Liou. Multi-Objective Optimization of Transonic Compressor Blade Using Evolutionary Algorithm. *Journal of Propulsion and Power*, 21(6):979-987, November-December 2005.
28. W. Liao and H. M. Tsai. Aerodynamic Design optimization by the Adjoint Equation Method on Overset Grids. In *AIAA Paper 2006-54, 44th AIAA Aerospace Science Meeting and Exhibit*, Reno, Nevada, USA, January 9-12 2006.
29. Efrén Mezura-Montes, editor. *Constraint-Handling in Evolutionary Optimization*, volume 198 of *Studies in Computational Intelligence*. Springer-Verlag, 2009.
30. B. Mialon, T. Fol, and C. Bonnaud. Aerodynamic Optimization Of Subsonic Flying Wing Configurations. In *AIAA-2002-2931, 20th AIAA Applied Aerodynamics Conference*, St. Louis Missouri, June 24-26 2002.
31. Shigeru Obayashi and Takanori Tsukahara. Comparison of Optimization Algorithms for Aerodynamic Shape Design. In *AIAA-96-2394-CP, AIAA 14th Applied Aerodynamics Conference*, New Orleans, LA, USA, June 17-20 1996.
32. Yew-Soon Ong, Prasanth B. Nair, and Kai Yew Lum. Max-min surrogate-assisted evolutionary algorithm for robust design. *IEEE Trans. Evolutionary Computation*, 10(4):392-404, 2006.
33. Akira Oyama. *Wing Design Using Evolutionary Algorithms*. PhD thesis, Department of Aeronautics and Space Engineering, Tohoku University, Sendai, Japan, March 2000.
34. Akira Oyama, Taku Nonomura, and Kozo Fujii. Data Mining of Pareto-Optimal Transonic Airfoil Shapes Using Proper Orthogonal Decomposition. *AIAA Journal Of Aircraft*, 47(5):1756-1762, September - October 2010.
35. Akira Oyama, Yoshiyuki Okabe, Koji Shimoyama, and Kozo Fujii. Aerodynamic Multiobjective Design Exploration of a Flapping Airfoil Using a Navier-Stokes Solver. *Journal Of Aerospace Computing, Information, and Communication*, 6(3):256-270, March 2009.
36. Kenneth V. Price, Rainer M. Storn, and Jouni A. Lampinen. *Differential Evolution. A Practical Approach to Global Optimization*. Springer, Berlin, 2005. ISBN 3-540-20950-6.
37. Man Mohan Rai. Robust Optimal Design With Differential Evolution. In *AIAA Paper 2004-4588, 10th AIAA/ISSMO Multidisciplinary Analysis and Optimization Conference*, Albany, New York, USA, 30 August - 1 September 2004.

38. T. Ray and H.M. Tsai. A Parallel Hybrid Optimization Algorithm for Robust Airfoil Design. In *AIAA Paper 2004-905, 42nd AIAA Aerospace Science Meeting and Exhibit*, Reno, Nevada, USA, 5–8 January 2004.
39. Margarita Reyes Sierra and Carlos A. Coello Coello. A Study of Fitness Inheritance and Approximation Techniques for Multi-Objective Particle Swarm Optimization. In *2005 IEEE Congress on Evolutionary Computation (CEC'2005)*, volume 1, pages 65–72, Edinburgh, Scotland, September 2005. IEEE Service Center.
40. Daisuke Sasaki and Shigeru Obayashi. Efficient search for trade-offs by adaptive range multi-objective genetic algorithm. *Journal Of Aerospace Computing, Information, and Communication*, 2(1):44–64, January 2005.
41. Daisuke Sasaki, Shigeru Obayashi, and Kazuhiro Nakahashi. Navier-Stokes Optimization of Supersonic Wings with Four Objectives Using Evolutionary Algorithms. *Journal Of Aircraft*, 39(4):621–629, July-August 2002.
42. Marc Secanell and Afzal Suleman. Numerical Evaluation of Optimization Algorithms for Low-Reynolds Number Aerodynamic Shape Optimization. *AIAA Journal*, 10:2262–2267, October 2005.
43. Koji Shimoyama, Akira Oyama, and Kozo Fujii. A New Efficient and Useful Robust Optimization Approach –Design for Multi-objective Six Sigma. In *2005 IEEE Congress on Evolutionary Computation (CEC'2005)*, volume 1, pages 950–957, Edinburgh, Scotland, September 2005. IEEE Service Center.
44. Koji Shimoyama, Akira Oyama, and Kozo Fujii. Development of Multi-Objective Six-Sigma Approach for Robust Design Optimization. *Journal Of Aerospace Computing, Information, and Communication*, 5(8):215–233, August 2008.
45. Helmut Sobieczky. Parametric Airfoils and Wings. In K. Fuji and G. S. Dulikravich, editors, *Notes on Numerical Fluid Mechanics, Vol.. 68*, pages 71–88, Wiesbaden, 1998. Vieweg Verlag.
46. Wenbin Song and Andy J. Keane. Surrogate-based aerodynamic shape optimization of a civil aircraft engine nacelle. *AIAA Journal*, 45(10):265–2574, October 2007. DOI: 10.2514/1.30015.
47. N. Srinivas and Kalyanmoy Deb. Multiobjective Optimization Using Nondominated Sorting in Genetic Algorithms. *Evolutionary Computation*, 2(3):221–248, Fall 1994.
48. András Szöllös, Miroslav Smíd, and Jaroslav Hájek. Aerodynamic optimization via multi-objective micro-genetic algorithm with range adaptation, knowledge-based reinitialization, crowding and epsilon-dominance. *Advances in Engineering Software*, 40(6):419–430, 2009.
49. Naoki Tani, Akira Oyama, Koichi Okita, and Nobuhira Yamanishi. Feasibility study of multi objective shape optimization for rocket engine turbopump blade design. In *44th AIAA/ASME/SAE/ASEE Joint Propulsion Conference & Exhibit*, Hartford, CT, 21 – 23 July 2008.
50. Shigeyoshi Tsutsui and Ashish Ghosh. Genetic algorithms with a robust solution searching scheme. *IEEE Trans. Evolutionary Computation*, 1(3):201–208, 1997.
51. Yoshihiro Yamaguchi and Toshiyuki Arima. Multi-Objective Optimization for the Transonic Compressor Stator Blade. In *AIAA Paper 2000-4909, 8th AIAA/USAF/NASA/ISSMO Symposium on Multidisciplinary Analysis and Optimization*, Long Beach, CA, USA, September 6 – 8 2000.
52. Qingfu Zhang and Hui Li. MOEA/D: A Multiobjective Evolutionary Algorithm Based on Decomposition. *IEEE Transactions on Evolutionary Computation*, 11(6):712–731, December 2007.
53. Eckart Zitzler and Lothar Thiele. Multiobjective Evolutionary Algorithms: A Comparative Case Study and the Strength Pareto Approach. *IEEE Transactions on Evolutionary Computation*, 3(4):257–271, November 1999.